NUCLEAR THEORY, Vol. 36 (2017)
eds. M. Gaidarov, N. Minkov, Heron Press, Sofia

Phases in an Algebraic Shell Model of Atomic Nuclei

K.P. Drumev[1], **A.I. Georgieva**[2], **J. Cseh**[3]

[1]Institute for Nuclear Research and Nuclear Energy,
Bulgarian Academy of Sciences, Sofia 1784, Bulgaria
[2]Institute of Electronics, Bulgarian Academy of Sciences, Sofia 1784, Bulgaria
[3]Institute of Nuclear Research, Hungarian Academy of Sciences, P.O. Box 51,
H-4001 Debrecen, Hungary

Abstract. We present results for the phase transition phenomenon in sd- and pf-shell nuclei from calculations performed in the symmetry-adapted basis of the Algebraic Microscopic Pairing-plus-Quadrupole Shell Model. Besides the quadrupole and the pairing (isoscalar plus isovector) interactions, the Hamiltonian also includes the spin-orbit interaction as single-particle terms of the studied systems. Comparison is made between the description obtained for the low-lying excitation energy spectra when these terms are present or not in the Hamiltonian.

1 Introduction

Symmetry-adapted nuclear models [1] are useful tools to explore nuclear systems. When a dynamical symmetry is present in the studied system, its description becomes incredibly simple. Usually, more than one such modes exist and they may simultaneously be present in the system as they compete, so one can explore the contribution of each of these simple limits into the resulting realistic behaviour of the system. A fundamental illustration of such an approach is presented by the algebraic structure of the shell model, where the long-range quadrupole-quadrupole interaction competes with different types (isovector and isoscalar) short-range interactions. The investigations of the possible dynamical symmetries in the microscopic Pairing-plus-Quadrupole Shell Model [2], led to establishing important connections between the groups generating the Hamiltonian of the model. These connections simplified the description of the influence of the different interactions on the energy spectra and transitions in realistic nuclei.

In the present work, we discuss a possible application of the Symmetry-Adapted Pairing-plus-Quadrupole Shell Model [2]. More specifically, we demonstrate how it can be applied to the description of properties of nuclei from the lower part of the sd shell and the lower pf shell. We also point out the possibility to effectively explore and describe the phases and phase transitions in these nuclei. We compare the results obtained when the spin-orbit term is included in

the Hamiltonian with the case when it is not. Furthermore, we investigate the effect of suppression of the isoscalar pairing.

2 The Algebraic Pairing-plus-Quadrupole Shell Model

The current approach uses a Hamiltonian that combines the quadrupole-quadrupole interaction with both the isoscalar and the isovector pairing terms. Other terms, like the spin-orbit interaction, may also be added. In earlier works [2–4], the important result that the spatial subalgebra $U(\Omega)$ of the shell-model algebra $U(4\Omega)$ contains two distinct dynamical symmetries defined by the reduction chains - one through $SO(\Omega)$ and another through $SU(3)$ was obtained. A direct connection between the pairing and the quadrupole bases was established which allowed the investigation of the influence of the short- and the long-range part of the residual interaction on the reproduction of the experimental energies of the nuclear systems.

In our study [2–4] of the algebraic structure of the shell-model algebra $U(4\Omega)$, the correspodence of the represantations of the microscopic pairing algebra $SO(\Omega)$ with the $SO(8)$-ones was used, since it contains all the limits of the $SO(8)-$ pairing model. The pair creation operators that appear in the Hamiltonian of this limit are: $S^\dagger_\mu = \sum_l \beta_l \sqrt{\frac{2l+1}{2}} [a^\dagger_{l\frac{1}{2}\frac{1}{2}} \times a^\dagger_{l\frac{1}{2}\frac{1}{2}}]^{010}_{0\mu 0}$ and $P^\dagger_\mu = \sum_l \beta_l \sqrt{\frac{2l+1}{2}} [a^\dagger_{l\frac{1}{2}\frac{1}{2}} \times a^\dagger_{l\frac{1}{2}\frac{1}{2}}]^{001}_{00\mu}$, where $\beta_l = +1$ or -1 are phase factors, and the bracket denotes the coupling in the angular momentum l, spin $s = 1/2$ and isospin $t = 1/2$ of the creation (annihilation) operators $a^\dagger_{l\frac{1}{2}\frac{1}{2}} (a_{l\frac{1}{2}\frac{1}{2}})$, of an individual nucleon. The pair annihilation operators can be obtained from these by Hermitian conjugation.

Elliott's $SU(3)$ algebra [5], generated by the components of the quadrupole operator: $Q_\mu = \sum_l \sqrt{8(2l+1)} (a^\dagger{}_{l\frac{1}{2}\frac{1}{2}} \times \tilde{a}_{l\frac{1}{2}\frac{1}{2}})^{(200)}_{(\mu 00)}$ and the angular momentum one: $L_\mu = \sum_l \sqrt{4l(2l+1)(l+1)/3} (a^\dagger{}_{l\frac{1}{2}\frac{1}{2}} \times \tilde{a}_{l\frac{1}{2}\frac{1}{2}})^{(100)}_{(\mu 00)}$, expressed in terms of the same operators $a^\dagger_{l\frac{1}{2}\frac{1}{2}} (a_{l\frac{1}{2}\frac{1}{2}})$ is also naturally contained in $U(\Omega)$. There exists a simple relation between the $SU(3)$ representation labels (λ,μ) and the shape parameters β, γ of the geometric model [6]. Hence, the $SU(3)$ classification of the many-body states has the advantage of allowing for a geometrical analysis of the eigenstates of a nuclear system. As a result, in $U(4\Omega)$ we obtain four reduction schemes, in which as distinct dynamical symmetries of the shell model algebra appear the $SU(3)$ algebra [6] and one of the branches of the $SO(8) \sim SO(\Omega)$ pairing algebra [7]. This allows the classification of the basis states of the system along each of them. The relation between these chains is established on the basis of the complementarity of the spatial dynamical symmetries in $U(\Omega)$ to the Wigner's spin-isospin $U_{ST}(4) \supset U_S(2) \otimes U_T(2)$ symmetry. This elucidates the algebraic structure of an extended Pairing-plus-Quadrupole Model, realized in the framework of the Elliott's SU(3) scheme [6].

Consequently, all chains determine full-basis sets and could be expressed through each other [2]. The eigenstates of the rotational limit of the model with quadrupole-quadrupole interaction are the basis states labeled by the quantum numbers of the representations (λ, μ) of the algebras in the SU(3) chain $|\Psi_R\rangle \equiv \left|\{f\}\alpha(\lambda,\mu)KL, \{\tilde{f}\}\beta(ST)M_T; JM\right\rangle$. Correspondingly, the basis states in which the pairing interaction is diagonal [7] are labeled as $|\Psi_P\rangle \equiv \left|\{f\}v[p_1,p_2,p_3]\xi L, \{\tilde{f}\}\beta(ST)M_T; JM\right\rangle$. In the above states, $\{f\}$ label the representations of $U(\Omega)$, $v[p_1, p_2, p_3]$ are the representations of the $SO(8)$ algebra, α, β, ξ, and K give the multiplicity labels of the corresponding reductions. Using the expansion of the pairing states in the $SU(3)$ basis states and the diagonalization procedure for its matrix in the $SU(3)$ basis, we obtain numerically the probability with which the states of the $SU(3)$ basis enter into the expansion of the pairing bases.

3 Phases and Phase Transitions between the Quadrupole−$SU(3)$ and the Pairing−$SO(8)$ Limits of the Model

3.1 Basis States and Hamiltonian

The basis states in which we perform our calculations

$$|\{(\lambda_\pi,\mu_\pi),(\lambda_\nu,\mu_\nu)\}\rho(\lambda,\mu)\kappa L, \{S_\pi, S_\nu\}S; JM\rangle \tag{1}$$

are built as $SU(3)$ proton (π) and neutron (ν) coupled configurations with well-defined particle number and good total angular momentum J.

We use a Hamiltonian with four ingredients of the form

$$H = \mathbf{G_0}\mathbf{S}^\dagger.\mathbf{S} + \mathbf{G_1}\mathbf{P}^\dagger.\mathbf{P} - \frac{\chi}{\mathbf{2}}\mathbf{Q}.\mathbf{Q} - \mathbf{C}\sum_{\mathbf{i}}\mathbf{l_i}.\mathbf{s_i}, \tag{2}$$

where the four parameters χ, $\mathbf{G_0}$, $\mathbf{G_1}$ and C are the strengths of the quadrupole-quadrupole, the isoscalar pairing, the isovector pairing and the single-particle spin-orbit term, respectively. The values of the four parameters (χ, G_0, G_1, and C) in (2) are determined from the fitting procedure. We also do three-parameter calculations where the spin-orbit term is not taken into account.

3.2 Phase Transitions on the Phase Diagrams

The relative weights of the interactions entering the eq. (2) serve as control parameters and define the phase diagram of the system (see Figure 1). In the case, when there are more than two dynamical symmetries, more than one control parameters should be introduced.

The quadrupole interaction has $SU(3)$ dynamical symmetry. Also, a simple model of the isovector and isoscalar pairing can be obtained in an L, S, T scheme

which has $SO(8)$ dynamical symmetry:

$$\begin{array}{ccccc} & & SO(8) & & \\ & \swarrow & \downarrow & \searrow & \\ SO_T(5)\otimes SO_S(3) & & SO(6) & & SO_S(5)\otimes SO_T(3) \\ & \searrow & \downarrow & \swarrow & \\ & & SO_T(3)\otimes SO_S(3) & & \end{array} \qquad (3)$$

From left to right these dynamical symmetries correspond to pure isovector interaction, pairing interaction with both isoscalar and isovector pairing with equal strengths, and only isoscalar pairing interactions, correspondingly. Next, the pairing-plus-quadrupole interactions define a submodel with a phase-space of two dimensions (two control parameters), which can be illustrated by a triangle. Each corner corresponds to a dynamical symmetry in the reduction of the spatial subspace of the shell model algebra $U(4\Omega)$: one of them is the $SU(3)$, and the others are each of the three limits (3) of the pairing algebra $SO(8)$. Hence, analytical solutions are available for the total pairing, with isoscalar and isovector interactions with equal strenghts, the pure isoscalar $SO_S(5)$ and for the pure isovector $SO_T(5)$ interactions [8]. Although the l.s term, compared to the other terms in the Hamiltonian does not belong to any dynamical symmetry, we may study how its presence changes the interplay between the rest of the terms in the Hamiltonian.

One possible convenient choice for the two control parameters in the Hamiltonian is to take x to represent the relative strength of the two kinds of pairing, so $G_0 = xG, G_1 = (1-x)G, 0 \leq x \leq 1$, and y to describe the relative weight of the quadrupole and the pairing strength G, so $\chi = y\chi_p, G = (1-y)\chi_p, 0 \leq y \leq 1$), where $\chi_p = \chi + G_0 + G_1$. As a result, the phase diagram is a triangle (see Figure 1(a)), where the three limiting cases at its vertices are defined by the conditions: $y = 1, x-$ arbitrary, for the $SU(3)$ limit, $x = 1, y = 0$ for the isoscalar case and $x = 0, y = 0$ for the isovector one. By means of their values we can evaluate the role of each of the three interactions in the description of the realistic nuclear spectra in each nucleus.

With the rise of the atomic number A and the increasing strength of the spin-orbit force, the $L-S$ coupling is destroyed by it and the system prefers the $j-j$ coupling. This adds a new dimension in the phase diagram which turns to a three-dimensional one, that can be illustrated by a tetrahedron (see Figure 1(b)). Then, the distance from the $L-S$ plain $(1-z)$ can be chosen as the third control parameter. This new control parameter z enters as $C = (1-z)\chi_{\max}$, $\chi_p = z\chi_{\max}$, where $0 \leq z \leq 1$. This last parameter, which is equal to the sum of the values of all parameters in the Hamiltonian (2) $\chi_{\max} = \chi + G_0 + G_1 + C$, is the scale parameter. Obviously, at $z = 1$ $C = 0$ and the two-parameter case (the triangle) is restored. At $z = 0$, only the $l.s$ term remains.

In the three-parameter case, when the spin-orbit interaction is not part of the Hamiltonian, the parametrization is made with two control parameters x and y

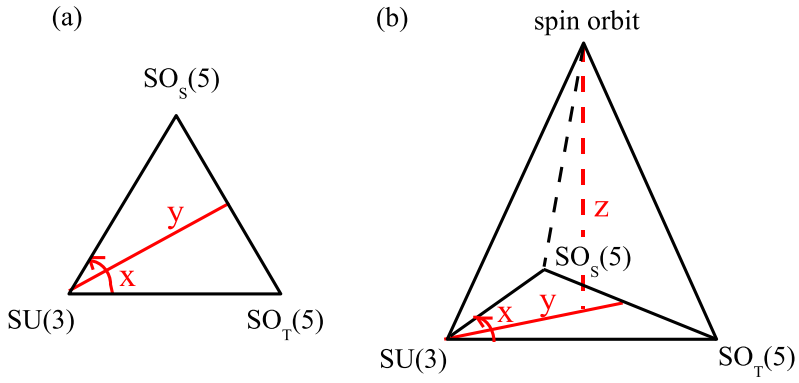

Figure 1. The two-parameter symmetry diagram (symmetry triangle) and the three-parameter symmetry diagram (symmetry tetrahedron).

which leads to the following form:

$$H = \chi_{\max}\{-\tfrac{y}{2}Q.Q + x(1-y)S^{\dagger}.S + (1-x)(1-y)P^{\dagger}.P\}. \quad (4)$$

When we include the spin-orbit interaction, introducing as a third control parameter z, the Hamiltonian (2) can be rewritten as

$$H = \chi_{\max}\{-\tfrac{yz}{2}Q.Q + x(1-y)zS^{\dagger}.S + (1-x)(1-y)zP^{\dagger}.P - (1-z)\textstyle\sum_i l_i.s_i)\}. \quad (5)$$

The above phase diagrams allow us to investigate the influence of these residual interactions on the spectra in real nuclear systems.

3.3 Choice of Nuclei and Calculation Procedure

The systems that we study are chosen according to the following criteria. First, we aim at full-space calculation with no truncations involved, so we try to keep the number of the valence particles reasonable. Moreover, we need a sufficient number of experimental values available for each nucleus in order for the fitting procedure to make sense. Our choice in this paper are the nuclei ^{20}Ne from the sd shell and ^{44}Ti from the pf shell. Both systems have two protons and two neutrons in their valence spaces.

The calculation procedure that we use consists of the following major steps. First, we generate [9] the admissible $SU(3)$ irreps for each type of particles. Then, we generate the $SU(3)$ basis and the Hamiltonian expressed in terms of $SU(3)$ tensors. Finally, we construct the matrix elements of the interactions [10] and search for the best description of the experimentally known lower-lying positive-parity energy states [11]. This is determined from a three (or four) parameter fit minimizing the RMS deviation $\sigma = \sqrt{\sum_i (E^i_{Th} - E^i_{Exp})^2/d}$ of our theoretical results (with $d = N - p$, where N - number of experimental

points, p- number of parameters in the fit). Finally, using these obtained results, we illustrate them with graphics for the behaviour of the quantities of interest.

4 Results

First, let us give the best-fit values obtained for both nuclei with the Hamiltonian (4). For ^{20}Ne, the values are $G_0^{best} = 0.29$ MeV, $G_1^{best} = 0.29$ MeV, $\chi^{best} = 0.11$ MeV, while for ^{44}Ti, we obtain $G_0^{best} = 0.11$, $G_1^{best} = 0.25$ MeV, $\chi^{best} = 0.02$ MeV. If the spin-orbit term is included in our calculation (when using the Hamiltonian (5)) then the best-fit result is obtained with a zero value for the isoscalar strength G_0. The values for the nucleus ^{20}Ne are $G_0^{best} = 0$, $G_1^{best} = 0.48$ MeV, $\chi^{best} = 0.12$ MeV, and $C^{best} = 3.36$ MeV, while for ^{44}Ti we obtain $G_0^{best} = 0$, $G_1^{best} = 0.29$ MeV, $\chi^{best} = 0.03$ MeV, and $C^{best} = 1.08$ MeV. We see that for these latter cases, the isoscalar pairing is eliminated from the description of both systems.

Figure 2 displays the dependence of energy excitation values on two control parameters when using the Hamiltonians (4) and (5). In all the pictures, the maximum value is achieved in the $SU(3)$ corner of the phase diagram. On the same figure, one can also see the position (denoted as a black dot) of the best-fit result which for ^{20}Ne lies at the values $x = 0.50$, $y = 0.16$ for the case of using the Hamiltonian (4) and $x = 0$, $y = 0.20$ for the Hamiltonian (5). For ^{44}Ti we obtain the result $x = 0.31$, $y = 0.05$ for the Hamiltonian (4) and $x = 0$, $y = 0.10$ for the Hamiltonian (5). These numbers confirm the more rotational nature of the nucleus ^{20}Ne compared to ^{44}Ti. The result from a calculation, performed for ^{20}Ne in [12] with a Hamiltonian similar to ours which lacks the proton-neutron pairing terms was used in [13] to extract the values of the control parameters which correspond to the best-fit outcome. The result differs from our outcome, where we obtain a point inside the symmetry diagram, so the pairing interaction is more strongly present.

Because of the symmetry non-conserving role of the spin-orbit term in the Hamiltonian, we choose to fix the parameter z and to study how the inclusion of this term affects the interplay between the rest of the present symmetries. So, we display the dependence of the excitation energy spectra on the two control parameters x and y with a value of the third parameter z obtained from the best-fit value for the spin-orbit strength (when included in the Hamiltoinan) and equal to zero (when it is not included).

The effect of suppression of the isoscalar pairing term when the spin-orbit interaction is present in the Hamiltonian has been noticed earlier [14]. The mechanism whereby this suppression takes place was discussed in detail in [15]. The effect may also be attributed to the similar character of the structure of the two operators as $SU(3)$ tensors.

Next, we can further present the results from Figure 2 in two simpler ways (or scenarios) for ^{20}Ne and ^{44}Ti:

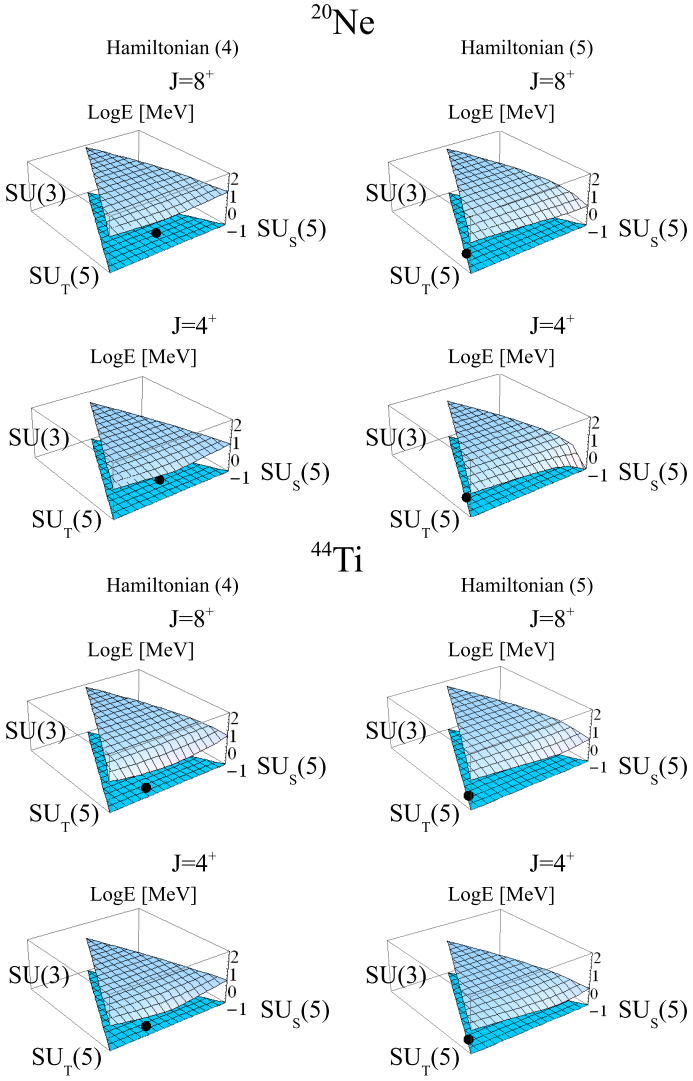

Figure 2. Three dimensional plots with results for the phase transitions in the $J = 4^+$ and $J = 8^+$ states from the ground-state band in the nuclei ^{20}Ne and ^{44}Ti. Results without the use of the spin-orbit term in the Hamiltonian are on the left while those obtained with the spin-orbit term included are on the right. The black dots show the point on the symmetry diagram for which the best-fit value in describing the excitation energy spectra is achieved.

(a) If we take $Q.Q$ and the spin-orbit interaction with strengths equal to the ones recommended by the best-fit result (i.e. fix the values for parameters y and z) and vary parameter x systematically;

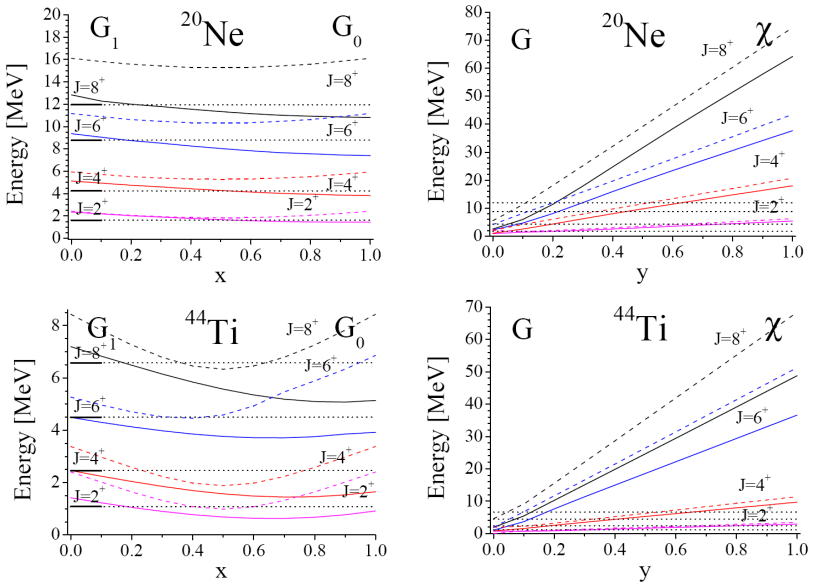

Figure 3. Excitation energies for the states from the ground-state band in the nuclei ^{20}Ne and ^{44}Ti. Results with the spin-orbit term in the Hamiltonain (full lines) are compared to the outcome obtained without the use of the spin-orbit term (dashed lines) and the experimental data [11] (dotted lines).

(b) If we take $x = 0.5$ (i.e. $G_0 = G_1$ - equal isovector and isoscalar pairing), fix the spin-orbit interaction (the value for the parameter z) and vary the values of the parameter y systematically.

These two choices can also be realized for the case of no spin-orbit terms present in the Hamiltonian.

In Figure 3 one can see a comparison of the result obtained with and without the use of the spin-orbit terms in the Hamiltonian. It is seen from the figure that for the ^{20}Ne in the sd shell, where the spatial symmetry group is $U(6)$ reducing directly to the "pairing" symmetry $O(6)$, which prescribes that both types of pairing enter with equal strengths $G_0 = G_1; x = 0.5$, the best-fit result gives exactly these values. Though it is not expected a priori. The inclusion of the spin-orbit interaction is not necessary for this shell, because an intruder level from the upper shell is not involved here. For the ^{44}Ti in the next pf shell this is not the case, since the $f_{7/2}$ level comes very low in energy, and is considered as a separate shell, which is due to some spin-orbit interaction. Even without it, $G_0 < G_1$ and it is eliminated by C. It must be noted that χ is much smaller in this case, and it is obvious that the g.s. band does not show a rotational behaviour. These effects are well reproduced by our approach.

5 Conclusions

We applied the Symmetry Adapted Pairing-plus-Quadrupole Shell Model to the description of low-lying positive-parity states of the $N = Z$ nuclei ^{20}Ne and ^{44}Ti from the lower sd and the lower pf shell. The Hamiltonian was expressed in terms of control parameters which allows us to study the interplay and the contribution of number of dynamical symmetries as phases. The difference between the more rotational character of the excitation spectrum of ^{20}Ne compared to the more vibrational one of ^{44}Ti, observed experimentally, is confirmed and illustrated by our results.

Acknowledgements

This work is supported by the Bulgarian National Foundation for Scientific Research under Grant Number DFNI-E02/6 (12.12.2014). It is also supported in part by the Hungarian Scientific Research Fund - OTKA (Grant No. K112962).

References

[1] P. Van Isacker, *Rep. Prog. Phys.* **62** (1999) 1661.

[2] K.P. Drumev, A.I. Georgieva, *Nuclear Theory* **32** (2013) 151, Proceedings of the 32 International Workshop on Nuclear Theory, 24-29 June 2013, eds. A. Georgieva, N. Minkov, Heron Press, Sofia.

[3] K.P. Drumev, A.I. Georgieva, *Nuclear Theory* **33** (2014) 162, Proceedings of the 33 International Workshop on Nuclear Theory, 22-28 June 2014, eds. A. Georgieva, N. Minkov, Heron Press, Sofia.

[4] K.P. Drumev, A.I. Georgieva, *Nuclear Theory* **34** (2015) 115, Proceedings of the 34 International Workshop on Nuclear Theory, 21-27 June 2015, eds. M. Gaidarov, N. Minkov, Heron Press, Sofia.

[5] J.P. Elliott, *Proc. Roy. Soc. London, Ser. A* **245** (1958) 128; **245** (1958) 562.

[6] J.P. Draayer, In: *Algebraic Approaches to Nuclear Structure: Interacting Boson and Fermion Models*, Contemporary Concepts in Physics VI, edited by R.F. Casten (Harwood Academic, Chur, Switzerland, 1993) 423.

[7] V.K.B. Kota, J.A. Castilho Alcaras, *Nucl. Phys.* **A764** (2006) 181.

[8] K.T. Hecht, *Ann. Rev. Nucl. Sci.* **23** (1973) 123.

[9] J.P. Draayer, Y. Leschber, S.C. Park, and R. Lopez, *Comput. Phys. Commun.* **56** (1989) 279.

[10] C. Bahri, J.P. Draayer, *Comput. Phys. Commun.* **83** (1994) 59; Y. Akiyama and J.P. Draayer, *Comput. Phys. Commun.* **5** (1973) 405.

[11] `http://www.nndc.bnl.gov/`

[12] C.E. Vargas, J. Hirsch, J.P. Draayer, *Nucl. Phys.* **A690** (2001) 409.

[13] J. Darai, J. Cseh, *J. Phys. Conf. Ser.* **580** (2015) 012057.

[14] Y. Lei, S. Pittel, N. Sandulescu, A. Poves, B. Thakur, and Y.M.Zhao, *Phys. Rev. C* **84** (2011) 044318.

[15] G.F. Bertsch and S. Baroni, arXiv:nucl-th/0904.2017v2.